International Journal of Engineering Materials and Manufacture (2019) 4(1) 15-21
https://doi.org/10.26776/ijemm.04.01.2019.02

Critical Assessment of Altitude Adaptive Dual Bell Nozzle using Computational Fluid Dynamics

Yeasir Mohammad Akib, Asif Kabir, and Mahdi Hasan

Received: 04 October 2018
Accepted: 30 December 2018
Published: 01 March 2019
Publisher: Deer Hill Publications

ABSTRACT
Space exploration and space tourism have now become a raging competition among the developed nations. For this reason, different types of advanced rocket nozzles with prospective privileges are introduced. Altitude adaptive dual bell nozzle will soon replace the conventional nozzles for the first stage rocket launcher. Indeed, this nozzle has auto adaption capability based on altitude. The major feature of a dual bell nozzle is the two bell-shaped contours separated by an inflection point. This nozzle has left rooms for researchers to test different flight conditions and transition characteristics. In this paper, a dual bell nozzle contour has been developed in MATLAB and analysed for different thermodynamic parameters. ANSYS Fluent is used in analysing flow through the nozzle. Shadowgraph imaging technique is used for measuring density gradient and compared it with fluent results. The simulations were performed by using the k-epsilon turbulence model.

Keywords: Altitude adaption, Dual bell nozzle, Supersonic flow, Inflection point, ANSYS Fluent

1 INTRODUCTION

Recently dual bell nozzle has been unearthed to be one of the most undertaking concepts. Plug nozzles, either linear or axisymmetric, nozzles with extendable exit cones (EEC), and dual-bell nozzles are presently under consideration by space industries and agencies as possible main engine candidates for future launchers [1, 2]. Currently, several research organizations (NASA, ONERA, etc.) and aviation and space industries (Boeing, Snecma Motors, Dassault, etc.) are working on the improvement of the performances and reliability of the supersonic rocket engine nozzles and space launchers nozzles [3].

The dual-bell concept was first initiated in literature in 1949 by F. Cowles and C. Foster, and was patented in the 1960s by Rocketdyne [4]. In 1994, Tests at Rocketdyne conducted by Horn and Fisher and in Europe by the Future European Space Transportation Investigations Program (FESTIP) at the European Space Agency (ESA) investigated the influence of the extension contour geometry on the flow behavior in the first experimental study and confirmed the feasibility of this nozzle design [4]. Horn and Fisher found that a dual-bell nozzle could provide enough thrust to carry 12.1% more payload than a conventional nozzle of the same area ratio [4]. Since the early nineties, many studies, mostly numerical, have been made by Goel and Jensen [5], Immich and Caporicci [6] (within the FESTIP program) to understand and attempted to predict the behavior of this new nozzle concept. A numerical study of the feasibility was made by Karl and Hagemann [7]. P. Goel and R. Jensen performed the first numerical analysis of dual-bell nozzles, which was published in 1995 [8]. Throughout the 2000s, several numerical and experimental studies of dual-bell nozzles were conducted in the United States and Europe [2].

Y. M. Akib[1], A. Kabir[2], and M. Hasan[3] ✉
[1]Department of Industrial and Production Engineering
Rajshahi University of Engineering and Technology (RUET)
Rajshahi-6204, Bangladesh

[2]Department of Mechanical Engineering
Bangladesh University of Engineering and Technology (BUET)
Dhaka, Bangladesh

[3]Department of Mechanical Engineering
North Carolina A&T State University, Greensboro, NC 27401, USA
E-mail: mhasan2@aggies.ncat.edu

Reference: Akib, Y. M., Kabir, A. and Hasan, M. (2019). Critical Assessment of Altitude Adaptive Dual Bell Nozzle using Computational Fluid Dynamic. *International Journal of Engineering Materials and Manufacture*, 4(1), 15-21.

A dual-bell nozzle has an inner base nozzle contour, a wall inflection, and an outer extension nozzle contour (Figure 1, left). This nozzle provides two stable operation modes. At low altitude, the high ambient pressure forces the flow to separate at the inflection (Figure 1, upper right) and at high altitude mode (Figure 1, lower right): the extension is flowing full, offering a large area ratio for improved altitude performances and this area ratio limitation of conventional nozzles is circumvented for an overall performance gain [9].

2 METHODOLOGY

At first, A full-length dual-bell nozzle contour is created using MATLAB. Then the meshing part is completed using ANSYS. For the analysis of this model FLUENT software is used. Along the nozzle flow behaviour is obtained. For the nozzle, air is taken as a working medium. Using the isentropic flow relations, area ratio of the dual-bell nozzle was determined. Due to the large assumed pressure and the high temperatures, the value of the ratio of specific heats was assumed to be 1.23.

2.1 Contour Design

Dual bell nozzle is defined by three section: converging part, throat and diverging part. Converging section and throat is designed using two circle equation having two different radii (Figure 2). This nozzle has two parts in its diverging section. The first part is known as the base or primary nozzle. The second bell (Figure 3) starts with a slope angle higher than the first bell end, such to yield an attached flow with a centred expansion at the inflection point in under expanded regime and a separated flow in the second bell in strong over expanded regime [13].

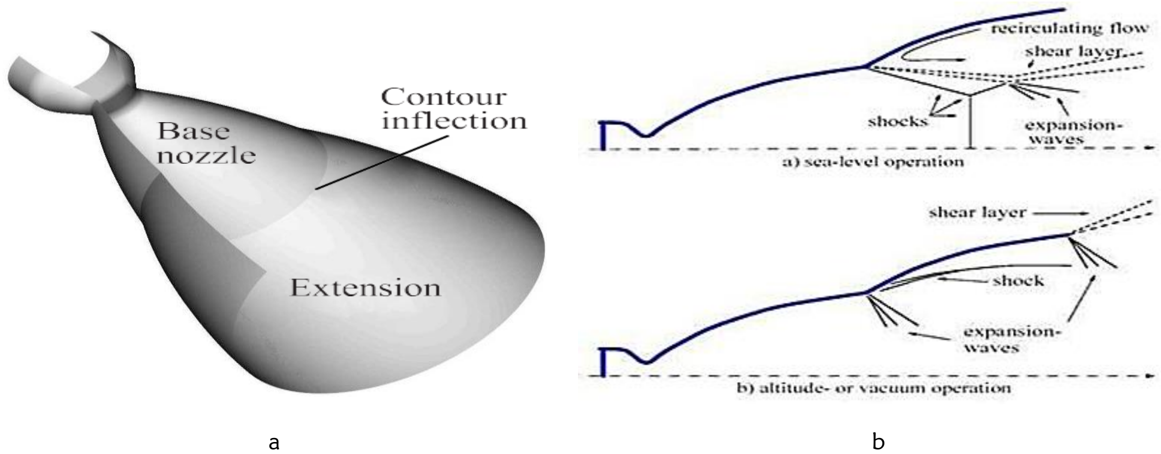

Figure 1: (a) Dual-bell nozzle (b) two operating modes: sea level (top) and altitude mode (bottom) [2]

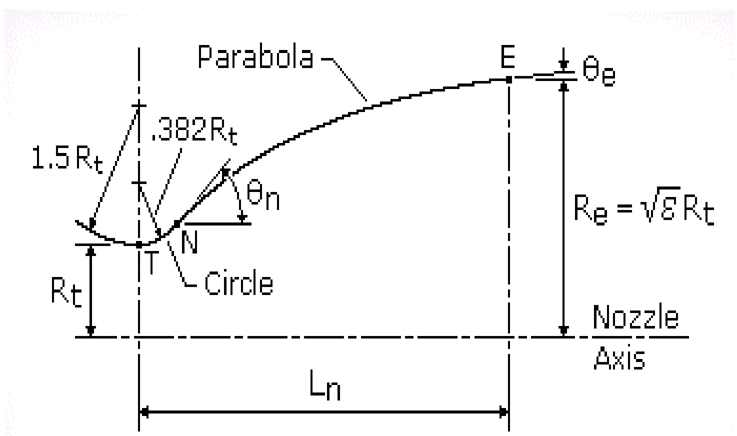

Figure 2: Dual bell nozzle (up to the first bell) [10]

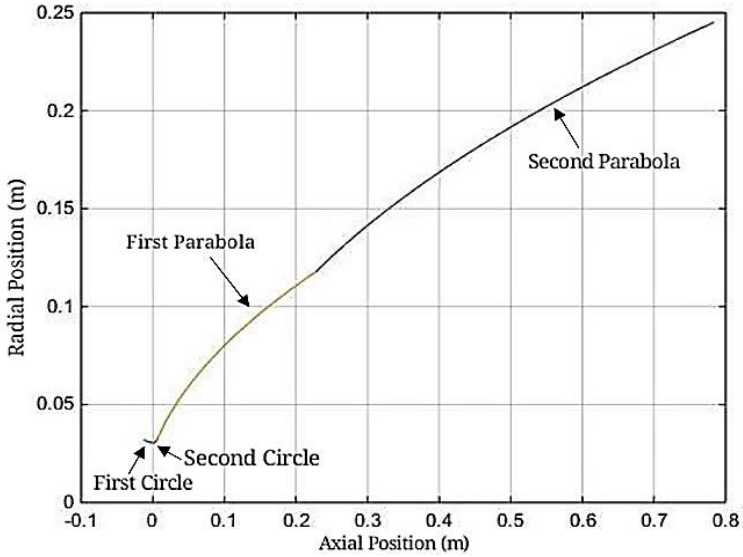

Figure 3: Dual bell nozzle with labeled section [11]

The first Parabola length of the nozzle is determined by

$$L_n = \frac{K(\sqrt{\varepsilon}-1)R_t}{\tan(\theta_e)} \quad (1)$$

Where K is a percentage of the length of an equivalent 15% conical nozzle, ε is nozzle exit ratio, R_t is the throat radius, θe is nozzle exit angle. A coordinate system is defined with the axial (x) axis and the radial (y) axis centred at the throat in order to define the nozzle further. The first and second curves define the entrance and exit of the throat of the nozzle and are based on circular curves. The third curve is a parabola. The equation of first parabola dual-bell is

$$x = ay^2 + by + c \quad (2)$$

The coefficients *a*, *b* and *c* are determined by the derivatives of the contour at the point where the circle from the throat meets the beginning of the parabola x_N, and the length of the nozzle L_n where the definition of x_N is

$$x_N = aR_N{}^2 + bR_N + c \quad (3)$$

Respectably the Slope of x_N and slope at the exit is

$$\frac{dy}{dx} = \tan(\theta_N) = \frac{1}{2aR_N + b} \quad (4)$$

$$\frac{dy}{dx} = \tan(\theta_e) = \frac{1}{2aR_e + b} \quad (5)$$

In matrix form, a full system of equations for the parabolic coefficients for the first parabola is

$$\begin{bmatrix} 2R_N & 1 & 0 \\ 2R_e & 1 & 0 \\ R_N{}^2 & R_N & 1 \end{bmatrix} \begin{bmatrix} a \\ b \\ c \end{bmatrix} = \begin{bmatrix} \frac{1}{\tan(\theta_N)} \\ \frac{1}{\tan(\theta_e)} \\ x_N \end{bmatrix} \quad (6)$$

Full Length of dual-bell nozzle is determined by

$$L_M = \frac{K_M(\sqrt{\varepsilon}-1)R_t}{\tan(\theta_e)} \quad (7)$$

Similarly, a full system of equations for the second parabola of the dual-bell nozzle

$$\begin{bmatrix} 2R_M & 1 & 0 \\ 2R_e & 1 & 0 \\ R_N{}^2 & R_N & 1 \end{bmatrix} \begin{bmatrix} a' \\ b' \\ c' \end{bmatrix} = \begin{bmatrix} \frac{1}{\tan(\theta_M)} \\ \frac{1}{\tan(\theta_e)} \\ x_M \end{bmatrix} \quad (8)$$

Where a', b' and c' are the coefficients of the second curve. The final design parameters are listed in Table 1.

Firstly, dual bell nozzle contour has developed in MATLAB using the above equation. Then the meshing part is completed using ANSYS FLUENT. A grid independent study was performed (Figure 4) by solving the governing equations for different grid densities ranging from 28,000 – 100,000 elements. The flow parameters at the nozzle exit for Pressure Ratio (PR) =50 show that the maximum difference between the results of the 48,000 and 100,00 portion Solver type was selected as density based, time was steady and 2D space was selected as axisymmetric. Hybrid initialization was selected as solution initialization and the data was computed from the pressure inlet. After running calculation, taking 3000 number of iteration, the isentropic parameter was calculated.

3 RESULTS AND DISCUSSIONS

3.1 Total Pressure

For both pressure ratio, 50 and 100, total pressure at the inlet is very high. Total pressure decreases slightly along the nozzle length but drops significantly from the midpoint of the second curve and becomes lowest at the exit. Total pressure varies from 17.5 kPa to 0.73 kPa at the exit region. Figure 5 exhibits the pressure variations across the nozzle for the two different pressure ratios.

3.2 Total Temperature

Total temperature variations along the nozzle length is shown below in figure 6. From the figures, the total temperature seems high from the starting point of the second curvature for both pressure ratios. After that, through the axial distance, temperature varies significantly. There is a slight variation in total temperature at the nozzle exit for the pressure ratios 50 and 100 .The temperature varies from 101-107 K as the exit gas meets the air at the exit portion.

3.3 Velocity Vector

Velocity vector for pressure ratios 50 and 100 are shown in figure 7. Velocity vectors show the change of Mach numbers along the nozzle geometry. For both the pressure ratio 50 and 100, velocity vector increases to become supersonic inside the nozzle and later decreases down to subsonic at the exit. This drastic decrement in velocity vector occurs after the second diverging section. For PR 100, the Mach velocity vector becomes slightly lower than PR 50.

Table 1: Parabolic coefficients of the dual-bell nozzle

Parabolic Coefficients	Dual-Bell Nozzle (First Contour)	Dual-Bell Nozzle (Second Contour)
a	10.2859	21.8315
B	0.5084	-4.7223
c	-0.0208	0.5362

Table 2: Design parameters for the dual-bell nozzle

Length (m)	Theta_N (degrees)	Theta_e (degrees)	Area Ratio
0.2732	20	9.588	64.5603

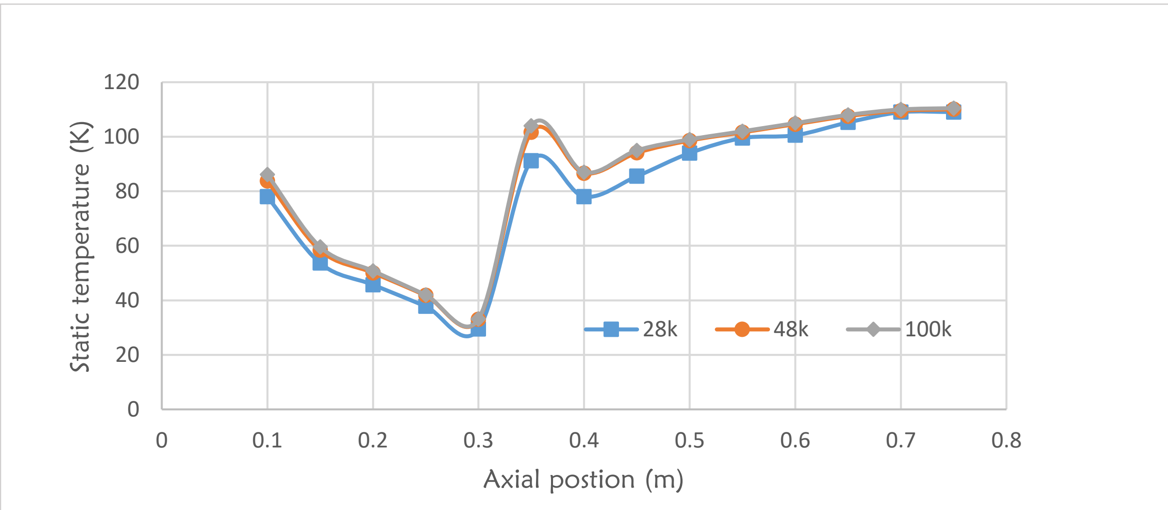

Figure 4: Grid independence test static temperature vs. axial position

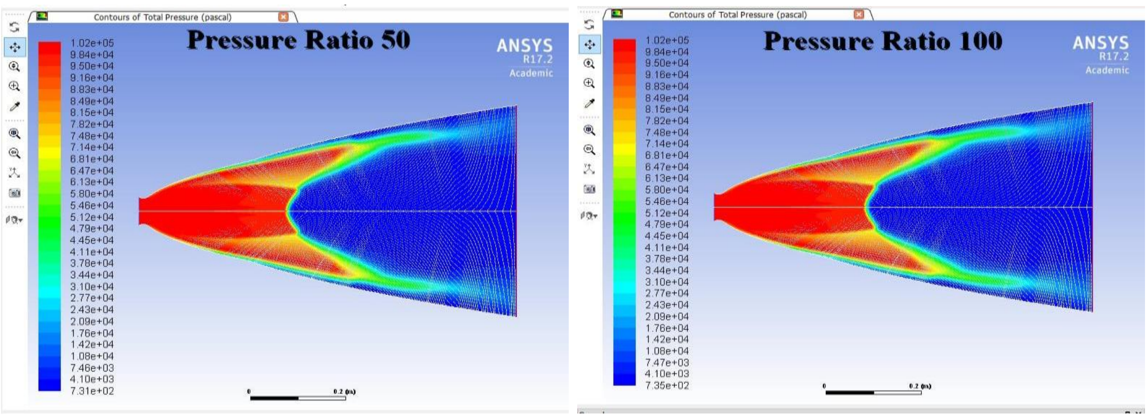

a b

Figure 5: Contour of total pressure for pressure ratio 50 (a) and 100 (b)

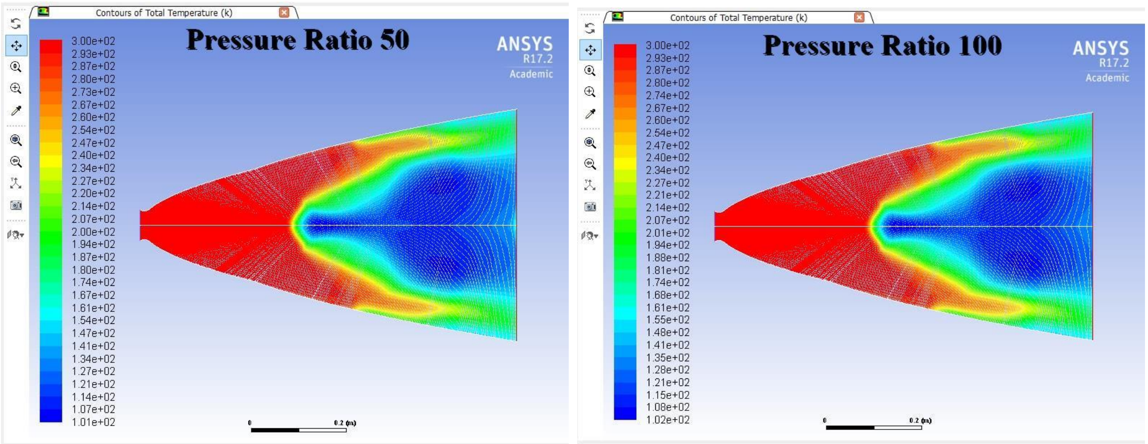

a b

Figure 6: Contour of total temperature for pressure ratio 50 (a) and 100 (b)

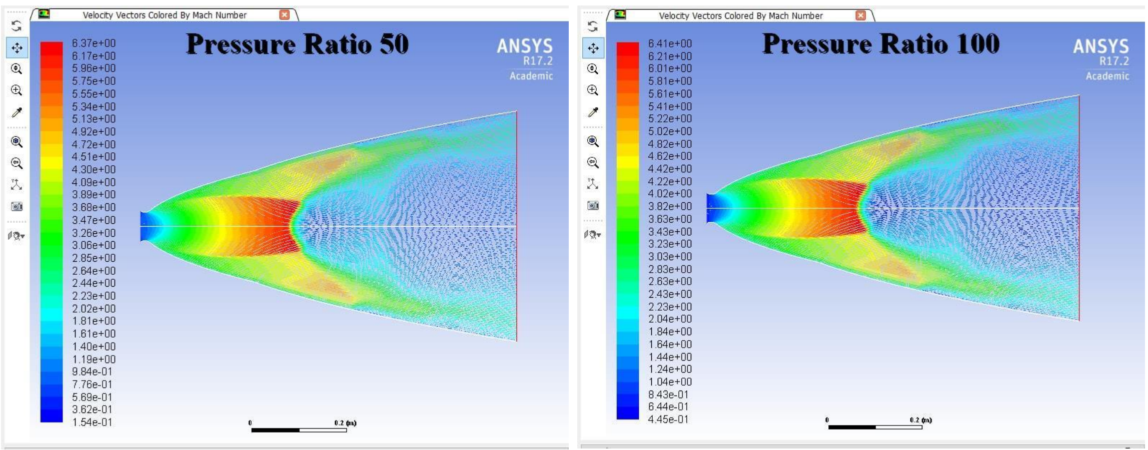

a b

Figure 7: Contour of Mach velocity vector for pressure ratio 50 (a) and 100 (b)

3.4 Mach Number

Mach number is subsonic at the inlet for both pressure ratio 50 and 100. Flow becomes supersonic and slightly hypersonic at the starting of the second diverging section. There are some variations of Mach number at the exit. At the midpoint of the second diverging section, PR 100 shows more variation of Mach number than PR 50.

3.5 Shadowgraph Visualization

Numerical shadowgraph or Schlieren image was generated by contour plotting the absolute value of the density gradient using Tecplot. The numerical shadowgraph did not distinguish between shocks or expansions since the absolute value was used.

Figure 10 shows the Mach number at specific positions of the nozzle for different pressure ratio. In the graph the yellow line represents the theoretical Mach number calculated from isentropic flow relation. For more consistency, our results are compared with numerical data at three different positions calculating by the Ref [12] only for Mach number. At throat and exit position, as the pressure ratio increases Mach number remains nearly same for both our own result and referred one. It can be noticed that at the inflection point, there is a little discrepancy in between that two numerical results.

4 CONCLUSIONS

A critical assessment of dual-bell nozzles was presented in this paper. This paper represents the design of a dual-bell nozzle contour and the study of the fluid parameters behaviour like pressure, temperature, Mach number, velocity vector etc. But in future studies, there are some aspects that may be studied. The present study was conducted only for four different pressure ratios. Future study may examine to perform some experimental works by using same input parameters to compare with the numerical data for validation.

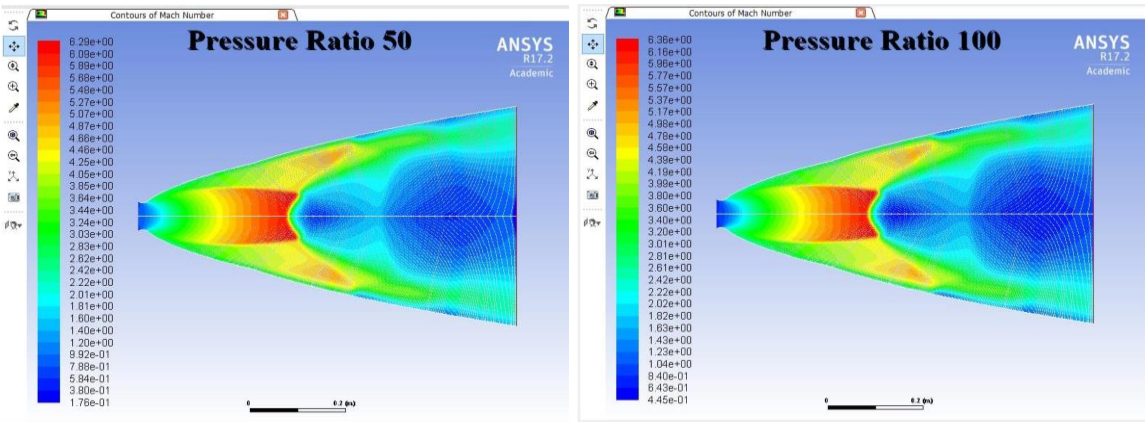

a b

Figure 8: Contour of Mach number for pressure ratio 50 (a) and 100 (b)

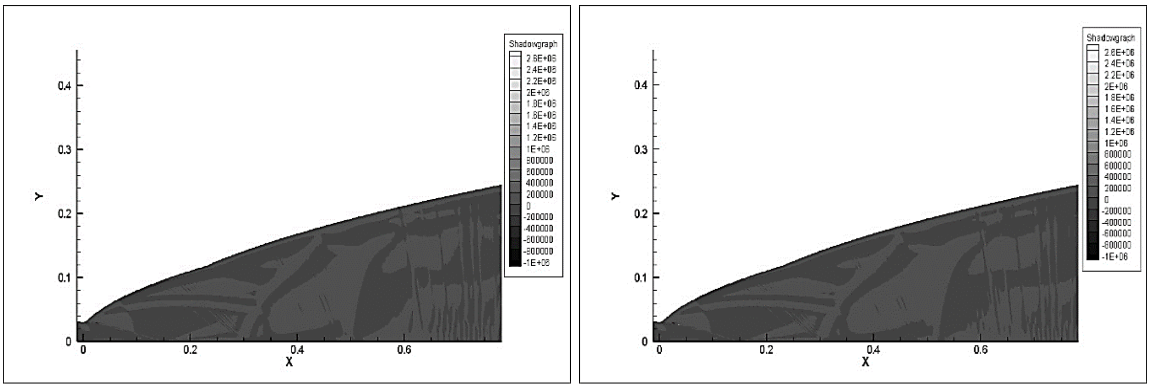

a b

Figure 9: Schlieren image or shadowgraph for pressure ratio 50 (a) and 100 (b)

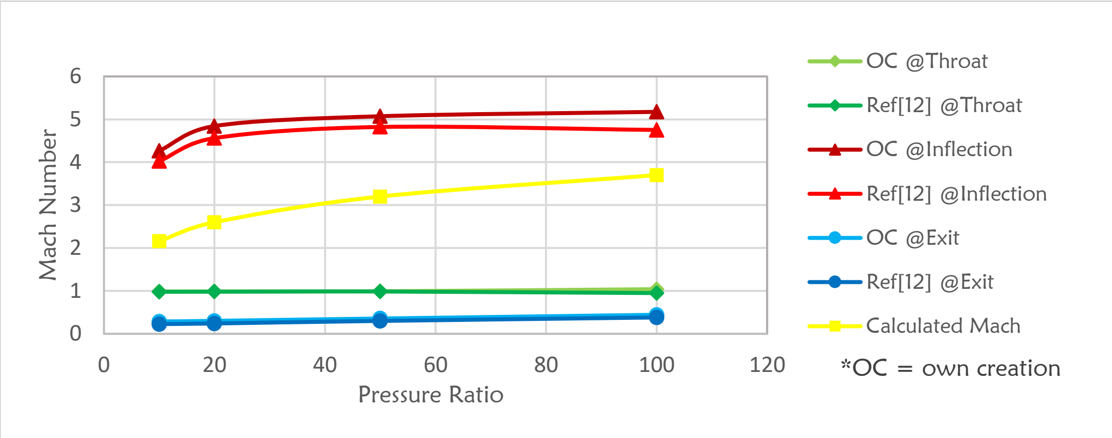

Figure 10: Mach number at different nozzle position (along with centre line) for four different pressure ratios

REFERENCES

1. Muss, J., Nhuyen, T., Reske, E., McDaniels, D., Muss, J., Nhuyen, T., Reske, E. & McDaniels, D. (1997, July). Evaluation of altitude compensating nozzle concepts for RLV. In *33rd Joint Propulsion Conference and Exhibit* (p. 3222).
2. Hagemann, G., Immich, H., Nguyen, T. V., & Dumnov, G. E. (1998). Advanced rocket nozzles. *Journal of Propulsion and Power*, *14*(5), 620-634.
3. Kbab, H., Sellam, M., Hamitouche, T., Bergheul, S., & Lagab, L. (2017). Design and performance evaluation of a dual bell nozzle. *Acta Astronautica*, *130*, 52-59.
4. Horn, M., & Fisher, S. (1993). Dual-bell altitude compensating nozzles. NASA Propulsion Engineering Research Center, 140-147.
5. Goel, P., & JENSEN, R. (1995). Numerical Analysis of the Performance of Altitude Compensating Dual Bell Nozzle Flows. In *Rockwell International Corp, 32nd JANNAF Combustion Subcommittee Meeting and Propulsion Engineering Research Centre 7th Annual Symposium p 117-140 (SEE N 96-27892 10-20).*
6. Immich, H., & Caporicci, M. (1997). FESTIP technology developments in liquid rocket propulsion for reusable launch vehicles. In *32nd Joint Propulsion Conference and Exhibit* (p. 3113).
7. Kronmüller, H., Schäfer, K., Stark, R., & Zimmermann, H. (2002). Kaltgas-Höhensimulationsprüfstand P6. 2 des DLR Lampoldshausen.
8. Frey, M., & Hagemann, G. (1999). Critical assessment of dual-bell nozzles. *Journal of propulsion and power*, *15*(1), 137-143.
9. Genin, C., Stark, R., Karl, S., & Schneider, D. (2012, July). Numerical investigation of dual bell nozzle flow field. In *48th AIAA/ASME/SAE/ASEE Joint Propulsion Conference & Exhibit* (p. 4164).
10. Kulhanek, S. L. (2012). *Design, Analysis, and Simulation of Rocket Propulsion System* (Doctoral dissertation, University of Kansas).
11. Akib, Y. M., Kabir, A., & Hasan, M. (2017). Characteristics Analysis of Dual Bell Nozzle using Computational Fluid Dynamics. In *3rd International Conference on Mechanical Industrial and Materials Engineering (ICMIME), 2017. Fluid Mechanics, FM-76.*
12. Davis, K., Fortner, E., Heard, M., McCallum, H., & Putzke, H. (2015). Experimental and computational investigation of a dual-bell nozzle. In *53rd AIAA Aerospace Sciences Meeting* (p. 0377).